

Synthesis and Growth of Au Nanostructures on MoS₂ Interface

T.I. Borodinova¹, V.I. Styopkin², A.A. Vasko², V.Ye. Kutsenko², O.A. Marchenko²

¹ F.D. Ovcharenko Institute of Biocolloid Chemistry, NAS of Ukraine, 42, Acad. Vernadsky Blvd., 03680 Kyiv, Ukraine

² Institute of Physics of NAS of Ukraine, 46, Nauka Ave., 03028 Kyiv, Ukraine

(Received 03 January 2018; revised manuscript received 14 June 2018; published online 25 June 2018)

Wet chemical synthesis gives wide possibilities for fabrication of noble metal nanoparticles (NP), which characteristics depend on many factors. The article is devoted to study of formation of Au nanostructures on MoS₂ substrate from growth solution, containing ethanol, ethylene glycol, glycerin, polyvinylpyrrolidone (PVP) and HAuCl₄. The study shows that obtained particles in this system are nearly spherical NP, wires, flat triangle and hexagonal nanoprisms (NPRs). NPs and dendritic structures growth without PVP and only presence of stabilizer leads to formation and further evolution of NPRs on MoS₂ substrate. For the first time it was also observed a growth of incomplete triangle and hexagonal NPRs, consisting of NP with size 50-100 nm. These incomplete nanoprisms transform to full shapes later on. Our experiments reveal that changing of component concentrations, ratio [PVP]/[HAuCl₄] and time of synthesis have a dominant influence on the shape of obtained NP. The possible mechanisms of NP growth on MoS₂ are discussed.

Keywords: Gold, Nanoparticles, Nanoprisms, Polyvinylpyrrolidone.

DOI: [10.21272/jnep.10\(3\).03017](https://doi.org/10.21272/jnep.10(3).03017)

PACS numbers: 61.46.Hk, 81.10.-h

1. INTRODUCTION

2D nanostructures have unique physical and chemical properties that open up possibilities of creation of new devices and materials. Such nanostructures can be easily obtained from layered materials, like graphite and transition metal dichalcogenides. More complex methods have to be used to produce 2D nanostructures of noble metals. One of them is surfactant-mediated synthesis on the basis of polyol method [1, 2], thermolysis with the use of template assisting [3].

Perspective template is the surface of MoS₂ monocrystal. Combination of Au nanostructures and sulfur-containing materials allow to manufacture promising devices that are widely used in photoluminescence [4-6], SERS [7-9], optoelectronic [10], photovoltaic devices [11], plasmonic organic solar cells [12], sensors [13], catalysis [14, 16], photoelectrochemical cells for water splitting [17], for the fabrication of rechargeable Li-O₂ batteries [18].

Advantage of MoS₂ template is possibility to produce Au nanostructures on a very thin sheet of MoS₂. It is demonstrated in [19] that if one accounts for interfacial energies and strains, the presence of misfit dislocations, and the compliance of the MoS₂ substrate, the experimentally observed growth orientation of Au nanostructures is favored despite the fact that it represents a larger elastic mismatch than two competing structures. The stability of the preferred orientation is attributed to the formation of a large number of strong Au-S bonds, and it is noted that this strong bond may serve as means to exfoliate and transfer large single layers of MoS₂.

There is very restricted number of studies of Au nanostructures on MoS₂ by using of wet chemical methods [9, 14]. This work is devoted to study of influence of components of growth media (ethanol, ethylene glycol, glycerin, polyvinylpyrrolidone, HAuCl₄), ratio of component concentrations C_{PVP}/C_{HAuCl_4} , time of synthesis and state of MoS₂ substrate on the shape, size and ori-

entation of Au nanostructures.

2. MATERIALS AND METHODS

To synthesize Au NPRs on investigated surfaces chloroauric acid (HAuCl₄ · 3H₂O, "Shanghai Synnad Fine Chemical Co., LTD"), ethyl alcohol, polyvinylpyrrolidone (29 kD, "Sigma-Aldrich"), ethylene glycol ("Reahim" Russian) and glycerin (manufactured Indonesia) were used.

The morphology of the Au nanostructures, their location on MoS₂ substrate were studied by scanning electron microscope (JSM-6060 microscope).

The influence of the growth medium components on investigated substrate was examined by wetting angle (WA) measurements. First, a droplet of each component was deposited on the freshly cleaved bare MoS₂ and on annealed Au (111) surfaces. Second, formation of a film of every component/combination of components of the growth medium were studied on the test substrates. Test substrates were immersed in a solution for 5-10 minutes, and after a droplet of deionized water was deposited on its surface. The same procedure was held with substrates immersed for 48 hours. The volume of droplets was equal to 2 μL. The value of the contact angle was averaged on the basis of 10 measurements. The error of measured wetting angle was within ± 5°.

3. THEORETICAL BACKGROUND

3.1 Growth Mechanisms of Au Structures

The growth mechanism of Au nanostructures under conditions of polyol synthesis can be considered within the LaMayer model [20]. At the first stage AuCl₄⁻ ions reduce to Au⁰. Thereafter, nuclei are formed in the places of maximum concentration of Au⁰. Every nucleus can decay if its size is less than critical or continue to grow if its size exceeds it. In the last stage augmentation in size of NPs is limited by diffusion of atoms from

free volume to the surface of Nps.

According to the different synthesis methods two main directions in explanation of plate-like structures exist. The first one deal with twin defects or stacking faults into the nanocrystals and the other highlights an important role of capping agents and their concentration in growth medium. For metals with fcc structure, e.g. Au, equilibrium shape of NPs is truncated octahedron [21]. Microprisms with the thickness up to 100 nm are far from this shape and have a large surface energy. To form such particles with a plate-like shape this symmetry has to be broken. In [22] and [23] authors supposed presence of twin defects or stacking faults into the nanocrystals.

NPs with minimal surface energy are obligatory to form twinned structures. The typical and most stable faces for bounding of Au and Ag NPs are {111} and {100}. Lofton and Sigmund showed that growth of these plate-like nanostructures strongly depends on twinned seeds. Such morphology of crystal leads to low energy reentrant grooves thus creating energetically favourable places for attachment of adatoms and lateral growth of crystal. Another deep theoretical and experimental study to confirm a paradigma of twinning processes was presented in [24]. The authors demonstrated that the probability of attachment of atom at the reentrant groove is 50 % times higher than at non-twinned site.

3.2 Capping Agents

Another mechanism supposed important role of capping agents (mainly surfactants) in formation of gold nanoplates. It was proposed that these agents have a preferential adsorption on (111) faces of gold crystals and supplies the shape of nanocrystals. There are lots of works which show using of PVP to establish shape of crystals. In [25] the thin nanoplates were obtained by realizing an effective two-dimensional (2D) crystal growth in a ternary surfactant mixture of cetyltrimethylammonium bromide (CTAB), polyvinylpyrrolidone (PVP), and polyethylene glycol (PEG). Different factors of chemical environment can drastically influence on final shape and size of Au NPs. Thus, in [26] it was revealed that shape of Au NP may be changed by the variation of solvent, containing PVP. Addition of NaBr to aqueous solution of PVP enhances growth of triangle flat NPs [27]. In [28] the morphology and dimension of Au NPs produced by use of aqueous thermal methodology strongly depended on the concentrations of the seed particles and CTAB, in addition to the concentration of Au ions (Au_3^+) and ascorbic acid. Therefore, triangle and star shapes were obtained at higher concentrations of Au seeds and reducing agent.

Synthesis of Au particles in presence of PVP slightly differs from those with CTAB, for example. Here, PVP binds Au ions, stabilizes nuclei/NPs from aggregation and determines morphology of NPs [29, 30]. Polymer is readily soluble in primary alcohols, where a highly hydrophilic hydrogen bond exists between the hydroxyl group of alcohols and the C-O group in the pyrrolidone ring of PVP molecules [26]. Catching of Au ions by polymer molecules leads to changing of PVP conformation to different loops and tangles that contain

Au ions [31]. Such polymer-metal ion complex promotes the reduction of Au_3^+ ions to Au_0 under soft conditions [32]. Note that Au ions join to polymer due to unshared electron pair of oxygen and nitrogen of pyrrolidone ring of PVP [33]. Thus, Au-PVP clusters can be formed.

On other hand, selective adsorption of PVP on crystallographic faces leads to different thickness of polymer layer and changes the rate of diffusion of atoms to growing surfaces. Using computer simulation surface energy ϕ was calculated for surfaces {111} and {100} of Au, Ag, Pd and Pt with and without adsorbed layer of PVP [34]. It was shown that the surface energy ϕ Au (100) of the faces {100} decreases after adsorption of α -pyrrolidone by 4.78 %, and for ϕ Au (111) – by 3.51 %. Under such conditions atoms predominantly join to the {100} faces and particles grow in the lateral direction while direction [111] is inhibited. Another respective study [35] demonstrates that PVP binds more strongly to Ag(100) than Ag(111) because of a surface-sensitive balance between direct binding and van der Waals attraction. Using density-functional theory (DFT) and molecular dynamics (MD) it was probed the adsorption-induced surface energies and spatially resolved binding of PVP monomer analogs on Au faces [36]. These calculations suggest that {111} facets should be prevalent in Au nanostructures grown with the help of PVP. Therefore, NPs grow with a plate-like shape.

3.3 Influence of MoS_2 Ssubstrate

The mechanism of growth of Au NPs is also likely connected with the redox reaction between MoS_2 and Au ions that is very good described in literature [37]. Formation of the redox pair $\text{AuCl}_4^-/\text{MoS}_2$ promotes reducing Au ions to Au_0 . Therefore, the common defect of MoS_2 substrate is valency-deficient sulphur leads to anchoring of gold atoms. As shown in [14, 15, 16] gold NPs nucleate preferentially at edges, line defects and cracks. Here, the largest number of broken S-bonds increase probability of attachment of AuCl_4^- ions [42]. The reduction of ions to Au_0 gives rise to formation of nuclei and their subsequent transformation to NPs.

In most cases, the highly energetic defect sites and coalescence of neighbouring particles produce intermediate, irregularly shaped particles that can be arranged in specific manner. In [38] MoS_2 surface serves as an effective template substrate in guiding the oriented growth of Au nanowires. Thus, using selected area electron diffraction peaks were observed for $\text{Au}\{220\} \parallel \text{MoS}_2$ (110), $\text{Au}\{311\} \parallel \text{MoS}_2$ (210), $\text{Au}\{111\} \parallel \text{MoS}_2$ (100), and $\text{Au}\{200\} \parallel \text{MoS}_2$ (310) showing the preferential directions of nanowires orientation. Our experimental results clearly demonstrate that substrate enforces oriented growth of Au structures, thus NPRs can be formed directly on solid interface.

4. RESULTS AND DISCUSSION

4.1 WA Measurements

Variation of constituents of multicomponent systems can drastically change a rate of reduction of Au ions in growth medium and as a resulting morphology of NPs. In addition, presence of a substrate create new centres of nucleation. Thus, we carried out SWA measurements

with test MoS₂ substrates to check the impact of components of growth medium on attachment of Au nuclei/NPs to the MoS₂ surface.

It is known that AuCl₄⁻ ions in a mixture of primary alcohols are reduced by ethanol at temperature $T = 80$ °C while ethylene glycol takes part in reduction processes only at high temperatures of synthesis ($T = 120$ - 195 °C) [41]. Our previous studies show that adding glycerin to the growth medium changes its viscosity and contributes to the formation of flat gold prisms.

Our results clearly show that PVP covers significant part of investigated substrate. The interaction with surface is most probably due to the hydrogen bonds of the amide - CONH₂ group of the pyrrolidone ring or methylene groups in the cycle and along backbone of PVP. Test experiments with MoS₂ immersed into solution ET + EG + G + PVP confirm it.

Surface wetting angle measurements demonstrated that for sample immersed into above solution for 10 min contact angle with deionized water equals 81 °. Its value is reduced to 60 ° for substrate immersed for 48 hours. We assume that such difference is due to compact packing of polymer on substrate interface.

Another type of WA experiments were performed with droplets of ET + EG + G + PVP and ET + EG + G + PVP + HAuCl₄ deposited on the freshly cleaved bare MoS₂ and on annealed Au(111) surfaces. Thus, all surfaces are equally well wetted ($< 9^\circ$). Results point out that it is not enough time for PVP to adsorb to the substrate while Au ions can easily attach to MoS₂ surface or get through thin layers of PVP and than bond with valency-deficient sulphur. Taking together, processes of adsorption of PVP on substrate undergo slower than attachment of Au ions to MoS₂ thus Au structures can be directly growth on substrate.

4.2 Au Decoration of MoS₂

Here, a series of experiments with varying time of synthesis and the ratio of HAuCl₄/PVP were carried out. A clear dependence between increasing these parameters and size, shape, quantity of the Au nanostructures was observed. When MoS₂ substrate is immersed into growth solution Au NPs decorate the substrate as shown in the SEM-images Fig. 1.

We found that NPs with clearly defined facets and complicated structure formed only in presence of PVP (see Fig. 1 d). Synthesis without PVP demonstrates growth of potato-like NPs (Fig. 1 a). Irregular-shaped flowers are observed along with dendritic outgrowths.

Our experimental results reveal that sophisticated and elegant morphology of flower-like NPs, as well as NPs with well-defined facets, drastically depends on ratio [PVP]/[HAuCl₄]. In [39] authors reported that Ag flower-like particles can be obtained by reducing silver nitrate with ascorbic acid in aqueous solutions.

The inherent growth anisotropy and surface imperfections of substrate make the assembly of NPs and the interactions between them direction-dependent. Here, side-defects (see insert Fig. 1 b) of MoS₂ play an important role in assembling NPs in an ordered manner – one can observe straight lines of dendrits in Fig. 1 c. Due to covering with PVP formation of cooperative in-

termolecular hydrogen bonding between its molecules leads to gluing NPs and further converting them to branching dendritic structures. Growth of these structures can be incited by valency-deficient sulphur. SEM-images of pair or groups of NPs clearly elucidate it (Fig. 1 b, Fig. 1 c).

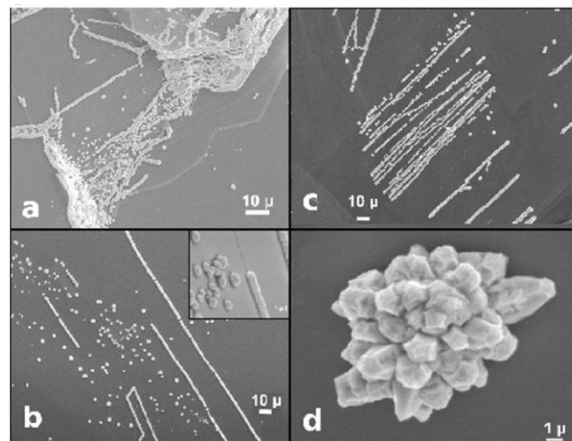


Fig. 1 – Dendrit outgrowths formed on substrate without PVP at $\tau = 5$ h and $C_{Au} = 0,125$ mM (a). $C_{Au} = 0,125$ mM, $C_{PVP} = 0,045$ M and time of synthesis $\tau = 5$ h (b). Insert in b demonstrates typical side defect of MoS₂. Straight lines of dendrits and flower-like NP at $\tau = 5$ h and $C_{Au} = 1$ mM, $C_{PVP} = 0,045$ M (c, d)

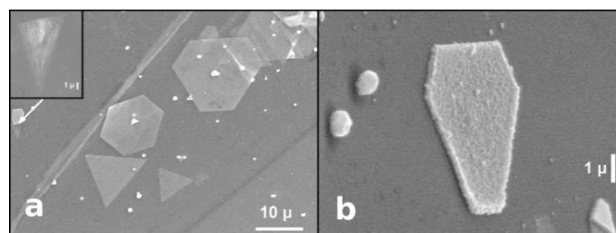


Fig. 2 – Au NPRs on MoS₂ substrate; synthesis parameters: $\tau = 48$ h, $C_{Au} = 1$ mM and $C_{PVP} = 0,045$ M. Arrow marks incomplete NPR (a). Hexagon NPR covered with PVP (b)

Keeping up a substrate in growth medium during 48 hours leads to formation of triangle and hexagon NPRs (see Fig. 2). The rough surface of some NPRs indicates presence a layer of PVP on it (Fig. 2 b). PVP is not always visible on substrate and Au structures, we observe only thick layers. At the first time also incomplete NPRs were observed in these experiments. In Fig. 2 a NPR is marked. Origin of this NPR is discussed in detail in the next section.

4.3 Growth of NPRs

When the MoS₂ plate is immersed in a growth medium containing HAuCl₄ and PVP several processes pass simultaneously on its surface: 1) binding of gold ions with valency-deficient sulphur; 2) adsorption of PVP from free volume (see SWA measurements); 3) binding of gold ions with PVP (Au-PVP clusters) in a free volume of growth media and their adsorption on substrate; 4) adhesion of gold prisms formed in free volume to the substrate. However, the last ones can be easily removed from surface by ultrasonic washing in distilled water. Nevertheless, after ultrasonic washing three types of gold prisms were identified on substrate:

incomplete prisms (Fig. 3 a, b), prisms with a smooth surface (Fig. 2 a; Fig. 3 c), and fortress like prisms (Fig. 4). How do Au NPRs form on the MoS₂ surface?

Incomplete prisms are structures that grow, form on MoS₂ surface and consist of a great number of NPs of different size. Specific arrangement of NPs in straight lines is direct impact of substrate. Their spontaneous growth depends on surface potential of substrate and local oversaturation of Au ions in energetically favourable places. Thus, some areas of prism can grow faster. Single NP or clusters can be attached to the surface or grow on it and became a structural part of NPRs in few ways: reduction of Au ions via MoS₂ and via ethanol. In [40] a multilayered MoS₂ substrate was immersed in growth medium consisting of N – methyl – pyrrolidinone + HAuCl₄ + NH₂OH for a set period of time. Here, authors confirmed that formation of NPs in straight lines with angular displacement of 60° is evidence of crystallographic deposition of metal nanostructures. Our experiments clearly demonstrate it (see Fig. 3).

Formation of incomplete prisms can be explained as follows (Fig. 3 c). Growth of nuclei undergoes simultaneously with the interaction of nanoclusters formed on the substrate and spontaneous agglomeration of gold atoms in the near-surface layer, their further coalescence and recrystallization. Such centers of “calm” nucleation are very few. Here, the close packing of nanoclusters can be occur due to PVP molecules [27]. The number of flat prisms with a smooth surface and typical lateral dimensions up to 10 μm is not high and their location is irregular on substrate. For such prisms oriented growth can be forced by crystal lattice of MoS₂.

SEM image in Fig. 3 c clearly demonstrates that gold structures consist of continuous areas of nuclei and chains of 50-100 nm NPs, lined parallel to faces of the prism. These structures were not observed under other conditions of synthesis and on other substrates.

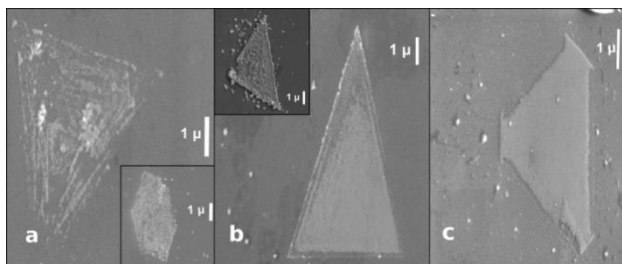


Fig. 3 – Stages of growth of triangle and hexagon NPRs on MoS₂ substrate (substrate was ultrasonically washed after growth process). NPRs with linear dimension of 10 μ consist of continuous areas of Au conglomerates and chains of NPs. Formation of single lines of NPs of triangle (enlarged image) and hexagon NPR (a), Formation of first layers of NPR (b) and (c). All samples are tilted at 60° to electron beam at study.

Another representative stage of growth of NPRs is depicted in Fig. 4. Here, both fortress-like prisms have completed inner part and brightly expressed perimeter.

Height of walls of hexagon fortress is approximately 250-300 nm. The inner surface of fortress is a thin layer of gold that reaffirmed via the change of the signal of secondary electrons along the lines A and B.

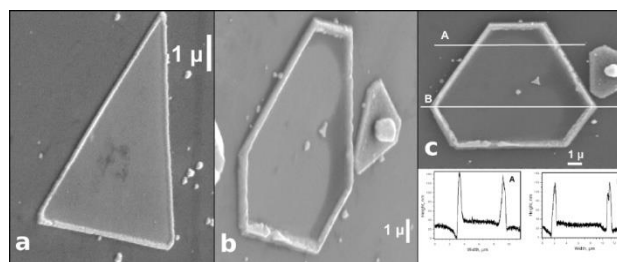


Fig. 4 – Triangle (a) and hexagon (b) fortress like NPRs with brightly expressed perimeter. In SEM-images a, b sample is tilted at 60° to electron beam. Front image of b with signals along lines A and B (c)

The growth of prisms can be considered as follows. At the first stage, 2D prisms are formed according to the tangential growth mechanism proposed by Kossel and Stranski, and then 3D structures are formed in the form of walls along the perimeter of prism. Why along the perimeter? It is known that supersaturation of atoms is greater at the vertices and edges than at a flat surface of NPR. Therefore, nucleation and growth of new layers are more likely appeared in such areas. Growth of single layer may not be yet ended while a new layer is already formed. For example, terraces are formed from unfinished atomic layers or as we called them above, the walls of the fortress.

5. CONCLUSIONS

Tuning of parameters of multi-compounded growth systems, i.e., molar ratio [PVP]/[HAuCl₄] and time of synthesis, allows to obtain structures with more complicated outer features, flower-like NPs, triangle and hexagon fortress like NPRs. It is shown that NPs and nanowires are formed at [PVP]/[HAuCl₄] = 1:45 during 5 hours while NPRs appear after 48 hours at the same conditions. Our experimental results indicate that PVP plays an important role as growth modifier of NPs and NPRs. Plate-like structures were preferentially formed on MoS₂ interface only in presence of polymer. Moreover, presence of all mentioned components of growth medium and substrate itself lead to formation of NPRs that allows to obtain a wide range of devices on base of Au nanostructures and MoS₂ interface.

CONFLICTS OF INTEREST

There are no conflicts to declare.

ACKNOWLEDGEMENTS

This research did not receive any specific grant from funding agencies in the public, commercial, or not-for-profit sectors.

Синтез та ріст наноструктур Au на інтерфейсі MoS₂Т.І. Бородінова¹, В.І. Стьопкін², А.А. Васько², В.Є. Куценко², О.А. Марченко²¹ Інститут біоколоїдної хімії ім. Ф.Д. Овчаренко Національної академії наук України, бульвар Академіка Вернадського, 42, 03680 Київ, Україна² Інститут Фізики НАН України, проспект Науки, 46, 03028 Київ, Україна

Синтез у водному середовищі надає широкі можливості для виготовлення наночастинок (НЧ) благородних металів, характеристики яких залежать від багатьох факторів. Стаття присвячена дослідженню росту наноструктур Au на підкладці MoS₂ у ростовому середовищі, що містить етанол, етиленгліколь, гліцерин, полівинілпіролідон (ПВП) та HAuCl₄. Наші дослідження показують, що морфологія отриманих НЧ є близькою до сферичної, дрогоподібною або у вигляді плоских трикутних/гексагональних нанопризм (НПР). Ріст НЧ та дендритоподібних структур може відбуватись і без ПВП, та лише наявність стабілізатора призводить до утворення та еволюції НПР на інтерфейсі MoS₂. Виявлено поетапний ріст незавершених трикутних і гексагональних НПР, що склалися з окремих НЧ розміром 50-100 нм. Такі структури перетворюються згодом у повноцінні НПР. Наші експерименти показують, що варіація концентрації компонентів, співвідношення [ПВП] / [HAuCl₄] та часу синтезу безпосередньо впливають на розмір та форму отриманих НЧ. Обговорюються можливі механізми росту отриманих структур Au на MoS₂.

Ключові слова: Золото, Наночастинки, Нанопризми, Полівинілпіролідон.

Синтез и рост наноструктур Au на интерфейсе MoS₂Т.И. Бородинова¹, В.И. Стьопкин², А.А. Васько², В.Е. Куценко², А.А. Марченко²¹ Институт биокolloидной химии им. Ф.Д. Овчаренко Национальной академии наук Украины, бульвар Академика Вернадского, 42, 03680 Киев, Украина² Институт Физики НАН Украины, проспект Науки, 46, 03028 Киев, Украина

Синтез в водной среде предоставляет широкие возможности для изготовления наночастиц (НЧ) благородных металлов, характеристики которых зависят от многих факторов. Статья посвящена исследованию роста наноструктур Au на подложке MoS₂ в ростовой среде, содержащей этанол, этиленгликоль, глицерин, поливинилпирролидон (ПВП) и HAuCl₄. Наши исследования показывают, что морфология полученных НЧ близка к сферической, проводоподобной или в виде плоских треугольных/ гексагональных нанопризм (НПР). Рост НЧ и дендритоподобных структур может происходить и без ПВП, и только наличие стабилизатора приводит к образованию и эволюции НПР на интерфейсе MoS₂. Наблюдается поэтапный рост незавершенных треугольных и гексагональных НПР, состоящих из отдельных НЧ размером 50-100 нм. Такие структуры превращаются со временем в полноценные НПР. Наши эксперименты показывают, что вариация концентрации компонентов, соотношения [ПВП] / [HAuCl₄] и времени синтеза непосредственно влияют на размер и форму синтезированных НЧ. Обсуждаются возможные механизмы роста полученных структур Au на MoS₂.

Ключевые слова: Золото, Наночастицы, Нанопризмы, Поливинилпирролидон.

REFERENCES

1. C. Li, W. Cai, B. Cao, F. Sun, Y. Li, C. Kan, L. Zhang, *Adv. Funct. Mater.* **16**, 83 (2006).
2. C. Wang, C. Kan, J. Zhu, X. Zeng, X. Wang, H. Li, D. Shi, *J. Nanomater.* **2010**, 969030 (2010).
3. B. Radha, G.U. Kulkarni, *Curr. Sci.* **102** No 1, 70 (2012).
4. S. Najmaei, A. Mlayah, A. Arbouet, C. Girard, J. Lotin, J. Lou, *ACS Nano* **8** No 12, 12682 (2014).
5. U. Bhanu, M.R. Islam, L. Tetard, S.I. Khondaker, *Sci. Rep.* **4**, 5575 (2014).
6. K.C.J Lee, Y.-H. Chen, H.-Y. Lin, C.-C. Cheng, P.-Y. Chen, T.-Y. Wu, M.-H. Shih, K.-H. Wei, L.-J. Li, C.-W. Chang, *Sci. Rep.* **5**, 16374 (2015).
7. S. Su, C. Zhang, L. Yuwen, J. Chao, X. Zuo, X. Liu, C. Song, C. Fan, L. Wang, *ACS Appl. Mater. Interf.* **6** No 21, 18735 (2014).
8. H. Zhou, F. Yu, C.F. Guo, Z. Wang, Y. Lan, G. Wang, Z. Fang, Y. Liu, S. Chen, L. Sun, Z. Ren, *Elec. Supp. Mater. (ESI) for Nanosc.* **7** No 20, 9153 (2015).
9. X. Yu, T. Shiraki, S. Yang, B. Ding, N. Nakashima, *RSC Adv.* **5**, 86558 (2015).
10. J. Miao, W. Hu, Y. Jing, W. Luo, L. Liao, A. Pan, S. Wu, J. Cheng, X. Chen, W. Lu, *Small* **11** No 20, 2392 (2015).
11. M.-K. Chuang, S.-S. Yang, F.-C. Chen, *Mater.* **8**, 5414 (2015).
12. X. Yang, W. Liu, M. Xiong, Y. Zhang, T. Liang, J. Yang, M. Xu, J. Ye, H. Chen, *J. Mater. Chem. A* **2**, 14798 (2014).
13. S. Su, H. Sun, F. Xu, L. Yuwen, C. Fan, L. Wang, *Microchim. Acta* **181**, 1497 (2014).
14. J. Kim, S. Byun, A.J. Smith, J. Yu, J. Huang, *J. Phys. Chem. Lett.* **4**, 1227 (2013).
15. A.Yu. Polyakov, L. Yadgarov, R. Popovitz-Biro, V.A. Lebedev, I. Pinkas, R. Rosentsveig, Y. Feldman, A.E. Goldt, E.A. Goodilin, *J. Phys. Chem. C* **118**, 2161 (2014).
16. X. Huang, Z. Zeng, S. Bao, M. Wang, X. Qi, Z. Fan, H. Zhang, *Nature. Comm.* **4**, 1444 (2013).
17. Z. Yin, B. Chen, M. Bosman, X. Cao, J. Chen, B. Zheng, H. Zhang, *Small.* **10**, 3537 (2014).
18. P. Zhang, X. Lu, Y. Huang, J. Deng, L. Zhang, F. Ding, Z. Su, G. Wei, O.G. Schmidt, *J. Mater. Chem. A* **3**, 14562

- (2015).
19. Y. Zhou, D. Kiriya, E.E. Haller, J.W. Ager, A. Javey, D.C. Chrzan, *Phys. Rev. B* **93**, 054106 (2016).
 20. V.K. LaMer, R.H. Dinegar, *J. Am. Chem. Soc.* **72** No 11, 4847 (1950).
 21. A.S. Barnard, X.M. Lin, L.A. Curtiss, *J. Phys. Chem. B* **109** No 51, 24465 (2005).
 22. Y. Xia, Y. Xiong, B. Lim, S.E. Skrabalak, *Angew Chem. Int Ed Engl.* **48** No 1, 60 (2009).
 23. C. Lofton, W. Sigmund., *Adv. Funct. Mater.* **15** No 7, 1197 (2005).
 24. R. Jagannathan, R.V. Mehta, J.A. Timmons, D.L. Black, *Phys. Rev. B* **48**, 13261 (1993).
 25. A.A. Umar, M. Oyama, M.M. Salleh, B.Y. Majli, *Cryst. Growth Des.* **10** No 8, 3694(2010).
 26. A. Kedia, P.S. Kumar, *J. Phys. Chem. C* **116**, 23721 (2012).
 27. M. Verma, A. Kedia, M.B. Newmai, P.S. Kumar, *RSC Adv.* **6** No 83, 80342 (2016).
 28. T.K. Sau, C.J. Murphy, *J. Am. Chem. Soc.* **126** No 28, 8648 (2004).
 29. K.M. Koczkur, S. Mourdikoudis, L. Polavarapu, S.E. Skrabalak, *Dalton Trans.* **44**, 17883 (2015).
 30. M. Grzelczak, J. Perez-Juste, P. Mulvaney, L.M. Liz-Marzan, *Chem. Soc. Rev.* **37**, 1783 (2008).
 31. T. Yao, Z. Sun, Y. Li, Z. Pan, H. Wei, Y. Xie, M. Nomura, Y. Niwa, W. Yan, Z. Wu, Y. Jiang, Q. Liu, S. Wei, *J. Am. Chem. Soc.* **132**, 7696 (2010).
 32. T. Yonezawa, N. Toshima, *J. Chem. Soc. Faraday Trans.* **91** No 22, 4111 (1995).
 33. T.I. BorodinoVA, V.I. Sapsay, V.R. Romanyuk, *J. Nano-Electron. Phys.* **7** No 1, 01032 (2015).
 34. W. Zhang, Y. Liu, R. Cao, Z. Li, Y. Zhang, Y. Tang, K. Fan, *J. Am. Chem. Soc.* **130** No 46, 15581 (2008).
 35. W.A. Al-Saidi, F. Haijun, K.A. Fichthorn, *Nano Lett.* **12** No 2, 997 (2012).
 36. S.-H. Liu, W.A. Saidi, Y. Zhou, K.A. Fichthorn, *J. Phys. Chem. C* **119** No 21, 11982 (2015).
 37. Y. Shi, J.-K. Huang, L. Jin, Y.-T. Hsu, S.F. Yu, L.-J. Li, H.Y. Yang, *Single Cryst. Sci. Rep.* **3**, 1839 (2013).
 38. D. Kiriya, Y. Zhou, C. Nelson, M. Hettick, S.R. Madhvapathy, K. Chen, P. Zhao, M. Tosun, A.M. Minor, D.C. Chrzan, A. Javey, *Adv. Funct. Mater.* **25**, 6257 (2015).
 39. L. Hongyan, L. Zhipeng, W. Wenzhong, W. Youshi, X. Hongxing, *Highly Adv. Mater.* **21** No 45, 4614 (2009).
 40. T.S. Sreeprasad, N. Phong, K. Namhooon, B. Vikas, *Nano Lett.* **13** No 9, 4434 (2013).
 41. S.E. Skrabalak, B.J. Wiley, M.H. Kim, E. Formo, Y. Xia, *Nano Lett.* **8**, 2077 (2008).
 42. I. Popov, G. Seifert, D. Tomanek, *Phys. Rev. Lett.* **108** No 15, 156802 (2012).